

**NANO EXPRESS**

**Open Access**

# Annealing effect on $\text{Sb}_2\text{S}_3\text{-TiO}_2$ nanostructures for solar cell applications

Yitan Li<sup>1</sup>, Lin Wei<sup>2</sup>, Ruizi Zhang<sup>1</sup>, Yanxue Chen<sup>1\*</sup>, Liangmo Mei<sup>1</sup> and Jun Jiao<sup>3,4</sup>

## Abstract

Nanostructures composed of vertical rutile  $\text{TiO}_2$  nanorod arrays and  $\text{Sb}_2\text{S}_3$  nanoparticles were prepared on an F:SnO<sub>2</sub> conductive glass by hydrothermal method and successive ionic layer adsorption and reaction method at low temperature.  $\text{Sb}_2\text{S}_3$ -sensitized  $\text{TiO}_2$  nanorod solar cells were assembled using the  $\text{Sb}_2\text{S}_3\text{-TiO}_2$  nanostructure as the photoanode and a polysulfide solution as an electrolyte. Annealing effects on the optical and photovoltaic properties of  $\text{Sb}_2\text{S}_3\text{-TiO}_2$  nanostructure were studied systematically. As the annealing temperatures increased, a regular red shift of the bandgap of  $\text{Sb}_2\text{S}_3$  nanoparticles was observed, where the bandgap decreased from 2.25 to 1.73 eV. At the same time, the photovoltaic conversion efficiency for the nanostructured solar cells increased from 0.46% up to 1.47% as a consequence of the annealing effect. This improvement can be explained by considering the changes in the morphology, the crystalline quality, and the optical properties caused by the annealing treatment.

**Keywords:**  $\text{TiO}_2$ ,  $\text{Sb}_2\text{S}_3$ , Nanorod, Solar cells, Annealing effect

## Background

Dye-sensitized solar cells (DSSCs) pioneered by O'Regan and Grätzel have been intensively investigated as a promising photovoltaic cell all over the world [1-5]. Until now, photovoltaic conversion efficiency of up to 11% has been reported for DSSCs in the laboratory [6]. Although the conversion efficiency is impressive, the expense of the dye required to sensitize the solar cell is still not feasible for practical applications. Therefore, it is critical to tailor the materials to be not only cost effective but also long lasting. Recently, the utilization of narrow-bandgap semiconductors as a light-absorbing material, in place of conventional dye molecules, has drawn much attention. Inorganic semiconductors have several advantages over conventional dyes: (1) The bandgap of semiconductor nanoparticles can be easily tuned by size over a wide range to match the solar spectrum. (2) Their large intrinsic dipole moments can lead to rapid charge separation and large extinction coefficient, which is known to reduce the dark current and increase the overall efficiency. (3) In addition, semiconductor sensitizers provide new

chances to utilize hot electrons to generate multiple charge carriers with a single photon. These properties make such inorganic narrow-bandgap semiconductors extremely attractive as materials for photovoltaic applications.

Recently, a range of nano-sized semiconductors has been investigated in photovoltaic applications including CdS [7-9], CdSe [10-13], Ag<sub>2</sub>S [14], In<sub>2</sub>S<sub>3</sub> [15], PbS [16],  $\text{Sb}_2\text{S}_3$  [17], Cu<sub>2</sub>O [18], as well as III-VI quantum ring [19]. Among these narrow-bandgap semiconductors,  $\text{Sb}_2\text{S}_3$  has shown much promise as an impressive sensitizer due to its reasonable bandgap of about 1.7 eV, exhibiting a strong absorption of the solar spectrum. The use of  $\text{Sb}_2\text{S}_3$  nanoparticles, which may produce more than one electron-hole pair per single absorbed photon (also known as multiple exciton generation), is a promising solution to enhance power conversion efficiency. Furthermore, the creation of a type-II heterojunction by growing  $\text{Sb}_2\text{S}_3$  nanoparticles on the  $\text{TiO}_2$  surface greatly enhances charge separation. All of these effects are known to increase the exciton concentration, lifetime of hot electrons, and therefore, the performance of sensitized solar cells. Limited research has previously been carried out with  $\text{Sb}_2\text{S}_3\text{-TiO}_2$  nanostructure for solar cell applications [20-22]. A remarkable performance was obtained in both liquid cell configuration and solid configuration. These

\* Correspondence: cyx@sdu.edu.cn

<sup>1</sup>School of Physics and State Key Laboratory of Crystal Materials, Shandong University, Jinan 250100, People's Republic of China

Full list of author information is available at the end of the article

findings were based on the use of porous nanocrystalline  $\text{TiO}_2$  particles; however, very little research has been conducted using single-crystalline  $\text{TiO}_2$  nanorod arrays. Compared with conventional porous polycrystalline  $\text{TiO}_2$  films, single-crystalline  $\text{TiO}_2$  nanorods grown directly on transparent conductive oxide electrodes provide an ideal alternative solution by avoiding particle-to-particle hopping that occurs in polycrystalline films, thereby increasing the photocurrent efficiency. Further enhancements in solid  $\text{Sb}_2\text{S}_3$ -sensitized solar cells demand a deeper understanding of the main parameters determining photoelectric behavior while also requiring additional research and insight into the electrical transporting process in these nanostructures.

In our present research study,  $\text{Sb}_2\text{S}_3$  semiconductor nanoparticles and single-crystalline rutile  $\text{TiO}_2$  nanorod arrays were combined to perform as a photoanode for a practical nanostructured solar cell (as depicted in Figure 1). The annealing effect on the photovoltaic performance and optical property of  $\text{Sb}_2\text{S}_3$ - $\text{TiO}_2$  nanostructures was studied systematically, and the optimal temperature of  $300^\circ\text{C}$  was confirmed. After annealing, apparent changes of morphological, optical, and photovoltaic properties were observed. The photovoltaic conversion efficiency of solar cell assembled using annealed  $\text{Sb}_2\text{S}_3$ - $\text{TiO}_2$  nanostructure demonstrated a significant increase of 219%, compared with that based on as-made  $\text{Sb}_2\text{S}_3$ - $\text{TiO}_2$  nanostructure.

## Methods

### Growth of single-crystalline rutile $\text{TiO}_2$ nanorod arrays by hydrothermal process

$\text{TiO}_2$  nanorod arrays were grown directly on fluorine-doped tin oxide (FTO)-coated glass using the following hydrothermal methods: 50 mL of deionized water was mixed with 40 mL of concentrated hydrochloric acid. After stirring at ambient temperature for 5 min, 400  $\mu\text{L}$  of titanium tetrachloride was added to the mixture. The feedstock, prepared as previously described, was injected into a stainless steel autoclave with a Teflon lining. The FTO substrates were ultrasonically cleaned for 10 min in a mixed solution of deionized water, acetone, and 2-

propanol with volume ratios of 1:1:1 and were placed at an angle against the Teflon liner wall with the conducting side facing down. The hydrothermal synthesis was performed by placing the autoclave in an oven and keeping it at  $180^\circ\text{C}$  for 2 h. After synthesis, the autoclave was cooled to room temperature under flowing water, and the FTO substrates were taken out, washed extensively with deionized water, and dried in open air.

### Deposition of $\text{Sb}_2\text{S}_3$ nanoparticles with successive ionic layer adsorption and reaction method and annealing treatment

Successive ionic layer adsorption and reaction (SILAR) method was used to prepare  $\text{Sb}_2\text{S}_3$  semiconductor nanoparticles. In a typical SILAR cycle, the F:SnO<sub>2</sub> conductive glass, pre-grown with  $\text{TiO}_2$  nanorod arrays, was dipped into the 0.1 M antimonite ethanol solution for 5 min at  $50^\circ\text{C}$ . Next, the F:SnO<sub>2</sub> conductive glass was rinsed with ethanol and then dipped in 0.2 M sodium thiosulfate solution for 5 min at  $80^\circ\text{C}$  and finally rinsed in water. This entire SILAR process was repeated for 10 cycles. After the SILAR process, samples were annealed in  $\text{N}_2$  flow at varied temperatures from  $100^\circ\text{C}$  to  $400^\circ\text{C}$  for 30 min. After annealing, a color change was noted in the  $\text{Sb}_2\text{S}_3$ - $\text{TiO}_2$  nanostructured samples, which were orange before annealing and gradually turned blackish as the annealing temperature increased.

### Characterization of the $\text{Sb}_2\text{S}_3$ - $\text{TiO}_2$ nanostructures

The crystal structure of the  $\text{Sb}_2\text{S}_3$ - $\text{TiO}_2$  samples were examined by X-ray diffraction (XD-3, PG Instruments Ltd., Beijing, China) with  $\text{CuK}\alpha$  radiation ( $\lambda = 0.154 \text{ nm}$ ) at a scan rate of  $2^\circ/\text{min}$ . X-ray tube voltage and current were set at 40 kV and 30 mA, respectively. The surface morphology of the  $\text{Sb}_2\text{S}_3$ - $\text{TiO}_2$  nanostructures was examined by scanning electron microscopy (SEM; FEI Sirion, FEI Company, Hillsboro, OR, USA). The optical absorption spectra were obtained using a dual beam UV-visible spectrometer (TU-1900, PG Instruments, Ltd.).

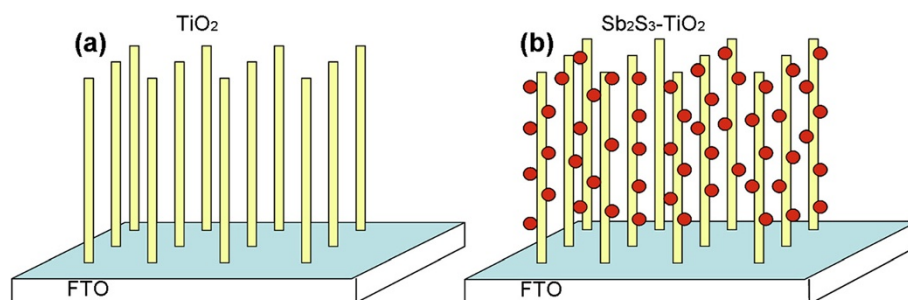


**Figure 1** Schematic of (a) bare  $\text{TiO}_2$  nanorod arrays on FTO and (b)  $\text{Sb}_2\text{S}_3$ - $\text{TiO}_2$  nanostructure on FTO.

### Solar cell assembly and performance measurement

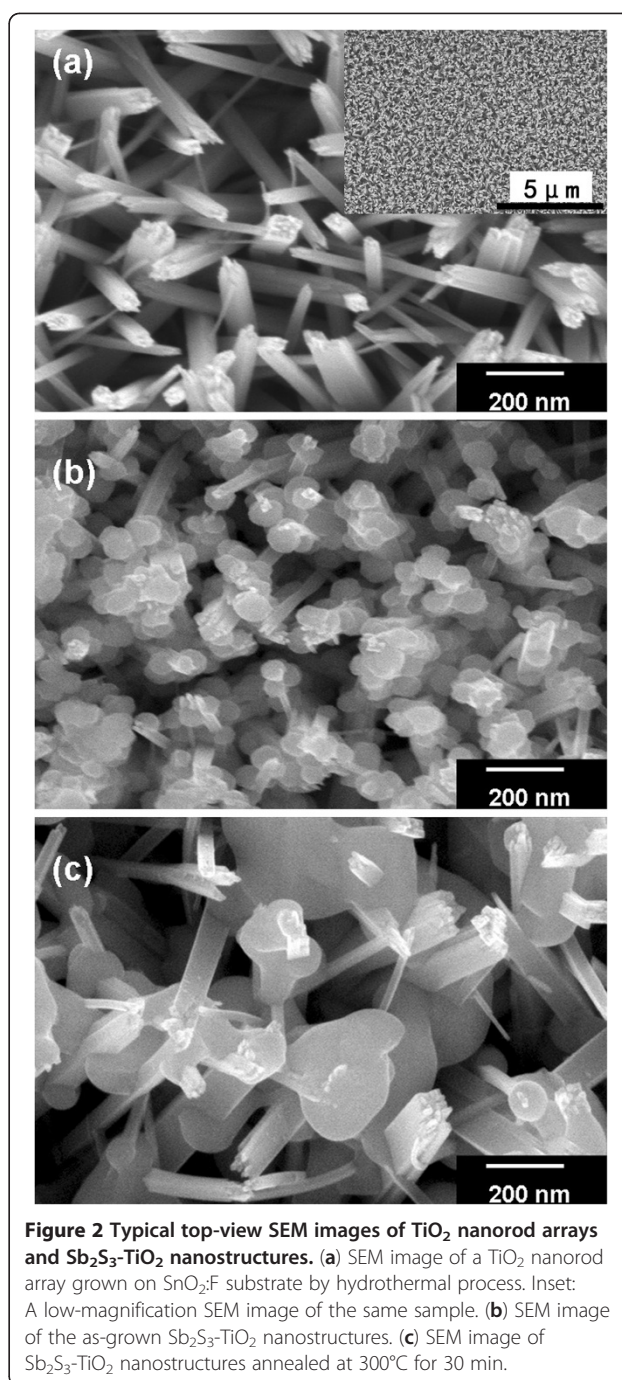
Solar cells were assembled using a  $\text{Sb}_2\text{S}_3$ - $\text{TiO}_2$  nanostructure as the photoanode. Pt counter electrodes were prepared by depositing an approximately 20-nm Pt film on FTO glass using magnetron sputtering. A 60- $\mu\text{m}$ -thick sealing material (SX-1170-60, Solaronix SA, Aubonne, Switzerland) with a  $3 \times 3$  mm aperture was pasted onto the Pt counter electrodes. The Pt counter electrode and the  $\text{Sb}_2\text{S}_3$ - $\text{TiO}_2$  sample were sandwiched and sealed with the conductive sides facing inward. A polysulfide electrolyte was injected into the space between the two electrodes. The polysulfide electrolyte was composed of 0.1 M sulfur, 1 M  $\text{Na}_2\text{S}$ , and 0.1 M NaOH which were dissolved in distilled water and stirred at 80°C for 2 h.

A solar simulator (Model 94022A, Newport, OH, USA) with an AM1.5 filter was used to illuminate the working solar cell at light intensity of one sun illumination (100  $\text{mW}/\text{cm}^2$ ). A source meter (2400, Keithley Instruments Inc., Cleveland, OH, USA) was used for electrical characterization during the measurements. The measurements were carried out using a calibrated OSI standard silicon solar photodiode.

## Results and discussion

### Morphology and crystal structure of $\text{Sb}_2\text{S}_3$ - $\text{TiO}_2$ nanostructure

The morphology of the rutile  $\text{TiO}_2$  nanorod arrays is shown in Figure 2a. The SEM images clearly show that the entire surface of the FTO glass substrate was uniformly covered with ordered  $\text{TiO}_2$  nanorods, and the nanorods were tetragonal in shape with square top facets. This nanorod array presented an easily accessed open structure for  $\text{Sb}_2\text{S}_3$  deposition and a higher hole transferring speed for the whole solar cell. No significant changes in nanorod array morphology were observed after annealing at 400°C. As-synthesized  $\text{Sb}_2\text{S}_3$ - $\text{TiO}_2$  nanostructure is shown in Figure 2b, indicating a combination of the  $\text{Sb}_2\text{S}_3$  nanoparticles and  $\text{TiO}_2$  nanorods. The  $\text{Sb}_2\text{S}_3$ - $\text{TiO}_2$  nanostructure after annealing at 300°C for 30 min is shown in Figure 2c. Compared to the CdS- $\text{TiO}_2$  nanostructure, in which 5- to 10-nm CdS nanoparticles distributed uniformly on the  $\text{TiO}_2$  nanorod [9], the as-deposited  $\text{Sb}_2\text{S}_3$  particles differed with a larger diameter of approximately 50 nm and often covered several  $\text{TiO}_2$  nanorods. This structural phenomenon was observed much more so in the annealed sample, where at least some melting of the low melting point (550°C)  $\text{Sb}_2\text{S}_3$  clearly occurred. After the annealing treatment, the size of  $\text{Sb}_2\text{S}_3$  particles increased, which enabled the  $\text{Sb}_2\text{S}_3$  particles to closely contact the  $\text{TiO}_2$  nanorod surface. This solid connection between  $\text{Sb}_2\text{S}_3$  nanoparticles and the  $\text{TiO}_2$  nanorods was beneficial to the charge separation and



improved the overall properties of the sensitized solar cells.

X-ray diffraction (XRD) patterns of the bare  $\text{TiO}_2$  nanorod array, the as-synthesized  $\text{Sb}_2\text{S}_3$ - $\text{TiO}_2$  nanostructure, and the annealed nanostructure are shown in Figure 3. Note in Figure 3a that the  $\text{TiO}_2$  nanorod arrays grown on the FTO-coated glass substrates had a tetragonal rutile structure (JCPDS no. 02-0494), which may be attributed to the small lattice mismatch between FTO and rutile. The as-

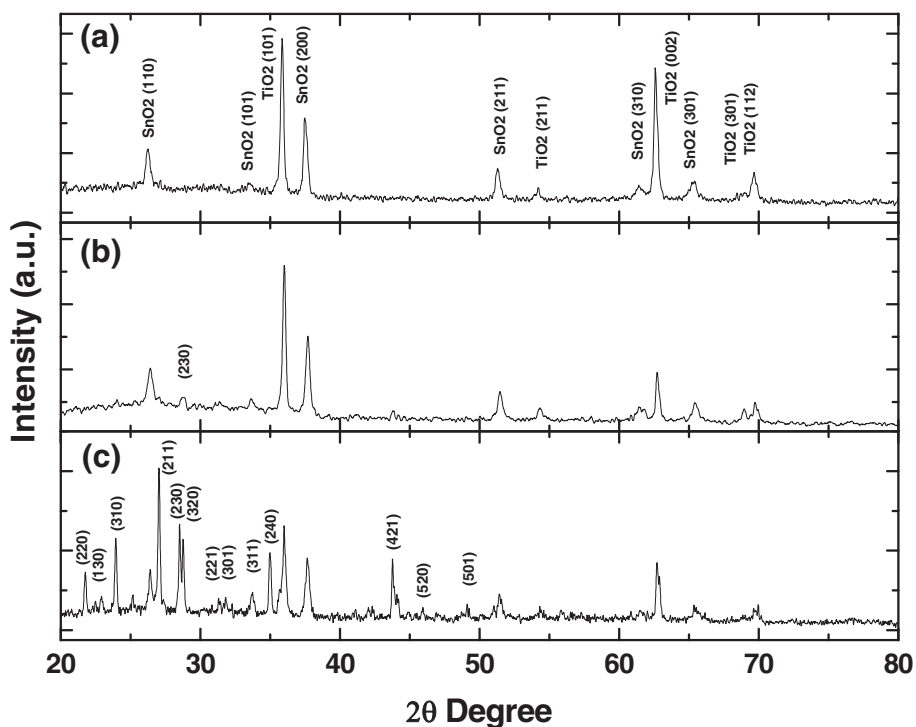


**Figure 3 XRD patterns.** The bare TiO<sub>2</sub> nanorod arrays (a), the as-grown Sb<sub>2</sub>S<sub>3</sub>-TiO<sub>2</sub> nanostructure electrode (b), and the annealed Sb<sub>2</sub>S<sub>3</sub>-TiO<sub>2</sub> nanostructure electrode under 300°C (c).

synthesized Sb<sub>2</sub>S<sub>3</sub>-TiO<sub>2</sub> nanostructure exhibited a weak diffraction peak (Figure 3b) at  $2\theta = 28.7^\circ$ , corresponding to the (230) plane of orthorhombic Sb<sub>2</sub>S<sub>3</sub>. As the annealing temperature increased, more diffraction peaks were observed, and the peaks became more distinct at the

same time. Figure 3c shows the XRD pattern of the nanostructure annealed at less than 300°C. All of the reflections were indexed to an orthorhombic phase of Sb<sub>2</sub>S<sub>3</sub> (JCPDS no. c-74-1046) [23]. The shape of the diffraction peaks indicates that the product was well crystallized.

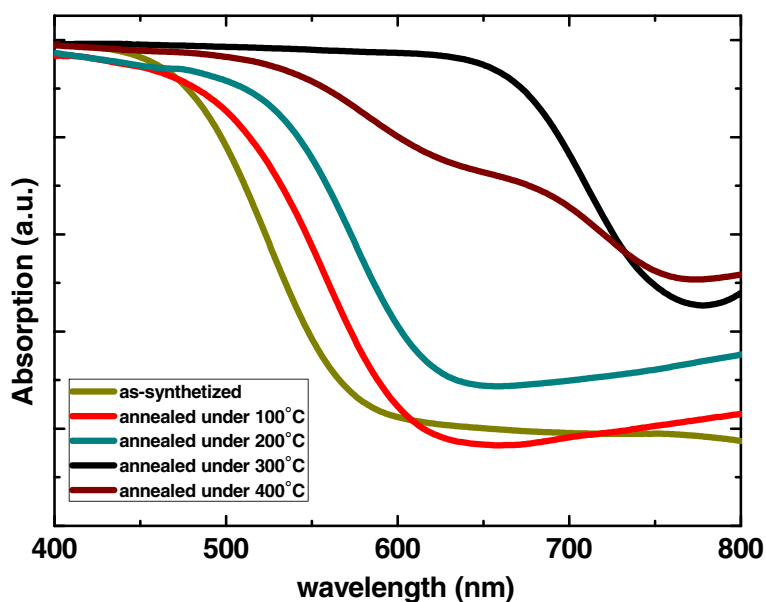


**Figure 4 Optical absorption spectra of Sb<sub>2</sub>S<sub>3</sub>-TiO<sub>2</sub> nanostructure samples.** Before (green spectrum) and after being annealed at 100°C (red spectrum), 200°C (blue-green spectrum), 300°C (black spectrum), and 400°C (brown spectrum).

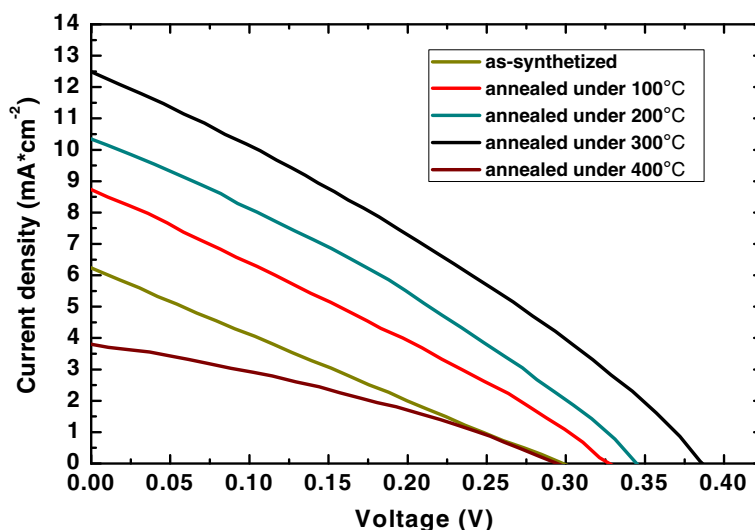


**Figure 5** *I-V* curves for the solar cells assembled using  $\text{Sb}_2\text{S}_3\text{-TiO}_2$  nanostructures annealed under varied temperature.

#### Optical property of the $\text{Sb}_2\text{S}_3\text{-TiO}_2$ nanostructures

The UV-visible absorption spectra of  $\text{Sb}_2\text{S}_3\text{-TiO}_2$  nanostructure samples are shown in Figure 4. An optical bandgap of 2.25 eV is estimated for the as-synthesized  $\text{Sb}_2\text{S}_3$  nanoparticles from the absorption spectra, which exhibits obvious blueshift compared with the value of bulk  $\text{Sb}_2\text{S}_3$ . After being annealed at 100°C, 200°C, and 300°C for 30 min, the bandgap of  $\text{Sb}_2\text{S}_3$  nanoparticles was red shifted to 2.19 eV (565 nm), 2.13 eV (583 nm), and 1.73 eV (716 nm), respectively. When annealed at 400°C, the absorption spectra deteriorated, which may be attributed to the oxidation as well as the evaporation of the  $\text{Sb}_2\text{S}_3$  nanoparticles. The  $\text{Sb}_2\text{S}_3\text{-TiO}_2$  nanostructure annealed at 300°C shows an enhanced absorption in the visible range, which is of great importance for solar cell applications and will result in higher power conversion efficiency. As shown by the XRD patterns and SEM images, this red shift in the annealed samples may be explained by the annealing-induced increase in particle size at the elevated temperatures. The annealing effect on the optical absorption spectra of bare  $\text{TiO}_2$  nanorod arrays was also studied (not included here). No obvious difference was found between the samples with and without annealing treatment. This result suggests that although annealing changes the morphology and crystallinity of  $\text{Sb}_2\text{S}_3$  nanoparticles, it does not significantly affect the optical property of  $\text{TiO}_2$  nanorod arrays.

#### Photovoltaic performance of the solar cell based on $\text{Sb}_2\text{S}_3\text{-TiO}_2$ nanostructure

The photocurrent-voltage (*I-V*) performances of the solar cells assembled using  $\text{Sb}_2\text{S}_3\text{-TiO}_2$  nanostructures annealed under different temperatures are shown in Figure 5. The *I-V* curves of the samples were measured

under one sun illumination (AM1.5, 100 mW/cm<sup>2</sup>). Compared with the solar cell based on as-grown  $\text{Sb}_2\text{S}_3\text{-TiO}_2$  nanostructure, the solar cell performances correspondingly improved as the annealing temperatures increased from 100°C to 300°C. The open-circuit voltage ( $V_{oc}$ ) improved from 0.3 up to 0.39 V, and the short-circuit current density ( $J_{sc}$ ) improved from 6.2 up to 12.1 mA/cm<sup>2</sup>. A power conversion efficiency of 1.47% for the sample with annealing treatment was obtained, indicating an increase of 219% (as compared to the 0.46% for the as-grown sample) as a consequence of the annealing treatment. The photovoltaic performance of annealed  $\text{Sb}_2\text{S}_3\text{-TiO}_2$  nanostructured solar cell under 400°C deteriorated, which coincides with the absorption spectrum. Detailed parameters of the solar cells extracted from the *I-V* characteristics are listed in Table 1.

This significant improvement of the photovoltaic performance obtained for annealed  $\text{Sb}_2\text{S}_3\text{-TiO}_2$  nanostructured solar cells is explained by the following reasons: (1) An enhanced absorption of sunlight caused by the red shift of the bandgap will result in an enhanced current density.

**Table 1** Parameters of  $\text{Sb}_2\text{S}_3\text{-TiO}_2$  nanostructured solar cells annealed at different temperatures

	$V_{oc}$ (V)	$J_{sc}$ (mA/cm <sup>2</sup> )	FF (%)	$\eta$ (%)
As-synthesized $\text{Sb}_2\text{S}_3\text{-TiO}_2$	0.30	6.10	0.25	0.46
$\text{Sb}_2\text{S}_3\text{-TiO}_2$ under 100°C	0.33	8.65	0.28	0.79
$\text{Sb}_2\text{S}_3\text{-TiO}_2$ under 200°C	0.34	10.32	0.31	1.10
$\text{Sb}_2\text{S}_3\text{-TiO}_2$ under 300°C	0.39	12.15	0.31	1.47
$\text{Sb}_2\text{S}_3\text{-TiO}_2$ under 400°C	0.29	3.82	0.32	0.36

$V_{oc}$ , open-circuit voltage;  $J_{sc}$ , integral photocurrent density; FF, fill factor;  $\eta$ , power conversion efficiency.

(2) Increase of  $\text{Sb}_2\text{S}_3$  grain size by annealing will reduce the particle-to-particle hopping of the photo-induced carrier. This hopping may occur in an as-grown nanostructure with  $\text{Sb}_2\text{S}_3$  nanoparticles. (3) Improvement of crystal quality of the  $\text{Sb}_2\text{S}_3$  nanoparticles by annealing treatment will decrease the internal defects, which can reduce the recombination of photoexcited carriers and result in higher power conversion efficiency. (4) Good contact between the  $\text{Sb}_2\text{S}_3$  nanoparticles and the  $\text{TiO}_2$  nanorod is formed as a result of high-temperature annealing. Such a superior interface between  $\text{TiO}_2$  and nanoparticles can inhibit the interfacial recombination of the injected electrons from  $\text{TiO}_2$  to the electrolyte, which is also responsible for its higher efficiency.

Our findings suggest the possible use of 3D nanostructure material grown by a facile hydrothermal method for sensitized solar cell studies. The drawback of this type of solar cell is a rather poor fill factor, which limits the energy conversion efficiency. This low fill factor may be ascribed to the lower hole recovery rate of the polysulfide electrolyte, which leads to a higher probability for charge recombination [24]. To further improve the efficiency of these nanorod array solar cells, we advise that a new hole transport medium with suitable redox potential and low electron recombination at the semiconductor and electrolyte interface should be developed. Moreover, as reported by Soel et al., other contributions such as the counter electrode material may also influence the fill factor [25].

## Conclusions

With a facile hydrothermal method, the single-crystalline  $\text{TiO}_2$  nanorod arrays were successfully grown on fluorine-doped tin oxide glass. Next,  $\text{Sb}_2\text{S}_3$  nanoparticles were deposited by successive ionic layer adsorption and reaction method to form a  $\text{Sb}_2\text{S}_3$ - $\text{TiO}_2$  nanostructure for solar cell applications. Annealing treatment was conducted under varied temperatures, and the optimal annealing temperature of 300°C was obtained. Obvious enhancement in visible light absorption was observed for the annealed samples. The photovoltaic performance for solar cells based on annealed  $\text{Sb}_2\text{S}_3$ - $\text{TiO}_2$  nanostructure shows an increase of up to 219% in power conversion efficiency.

## Competing interests

The authors declare that they have no competing interests.

## Authors' contributions

YL carried out the preparation of  $\text{Sb}_2\text{S}_3$ - $\text{TiO}_2$  nanostructured solar cells and drafted the manuscript. LW conducted the optical absorption spectra and the *I-V* measurements. RZ carried out the preparation of  $\text{TiO}_2$  nanorod arrays and the XRD measurements. YC carried out the SEM characterization and supervised the work. LM and JJ analyzed the results and finalized the manuscript. All authors read and approved the final manuscript.

## Acknowledgments

This work was supported by the National Key Basic Research Program of China (2013CB922303, 2010CB833103), the National Natural Science Foundation of China (60976073, 11274201, 51231007), the 111 Project (B13029), the National Found for Fostering Talents of Basic Science (J1103212), and the Foundation for Outstanding Young Scientist in Shandong Province (BS2010CL036).

## Author details

<sup>1</sup>School of Physics and State Key Laboratory of Crystal Materials, Shandong University, Jinan 250100, People's Republic of China. <sup>2</sup>School of Information Science and Engineering, Shandong University, Jinan 250100, People's Republic of China. <sup>3</sup>Department of Mechanical and Materials Engineering, Portland State University, P.O. Box 751, Portland, OR 97207-0751, USA. <sup>4</sup>Department of Physics, Portland State University, P.O. Box 751, Portland, OR 97207-0751, USA.

Received: 31 October 2012 Accepted: 9 February 2013

Published: 19 February 2013

## References

1. O'Regan B, Grätzel M: A low-cost, high-efficiency solar-cell based on dye-sensitized colloidal  $\text{TiO}_2$  films. *Nature* 1991, **353**:737.
2. Grätzel M: Photoelectrochemical cells. *Nature* 2001, **414**:338.
3. Kao MC, Chen HZ, Young SL, Lin CC, Kung CY: Structure and photovoltaic properties of  $\text{ZnO}$  nanowire for dye-sensitized solar cells. *Nanoscale Res Lett* 2012, **7**:260.
4. Lu LY, Chen JJ, Li LJ, Wang WY: Direct synthesis of vertically aligned  $\text{ZnO}$  nanowires on FTO substrates using a CVD method and the improvement of photovoltaic performance. *Nanoscale Res Lett* 2012, **7**:293.
5. Hossain MF, Zhang ZH, Takahashi T: Novel micro-ring structured  $\text{ZnO}$  photoelectrode for dye-sensitized solar cell. *Nano-Micro Lett* 2010, **2**:53.
6. Yasuo C, Ashrafali I, Yuki W, Ryoichi K, Naoki K, HAN LY: Dye-sensitized solar cells with conversion efficiency of 11.1%. *Jpn J Appl Phys* 2006, **45**:638.
7. Sun WT, Yu Y, Pan HY, Gao XF, Chen Q, Peng LM:  $\text{CdS}$  quantum dots sensitized  $\text{TiO}_2$  nanotube-array photoelectrodes. *J Am Chem Soc* 2008, **130**:1125.
8. Zhu G, Su FF, Lv T, Pan LK, Sun Z: Au nanoparticles as interfacial layer for  $\text{CdS}$  quantum dot-sensitized solar cells. *Nanoscale Res Lett* 2010, **5**:1749.
9. Wang CB, Jiang ZF, Wei L, Chen YX, Jiao J, Eastman M, Liu H: Photosensitization of  $\text{TiO}_2$  nanorods with  $\text{CdS}$  quantum dots for photovoltaic applications: a wet-chemical approach. *Nano Energy* 2012, **1**:440.
10. Zhang QX, Guo XZ, Huang XM, Huang SQ, Li DM, Luo YH, Shen Q, Toyoda T, Meng QB: Highly efficient  $\text{CdS}/\text{CdSe}$ -sensitized solar cells controlled by the structural properties of compact porous  $\text{TiO}_2$  photoelectrodes. *Phys Chem Chem Phys* 2011, **13**:4659.
11. Luan CY, Aleksandar V, Andrei SS, Xu XQ, Wang HE, Chen X, Xu J, Zhang WJ, Lee CS, Andrey LR, Juan AZ: Facile solution growth of vertically aligned  $\text{ZnO}$  nanorods sensitized with aqueous  $\text{CdS}$  and  $\text{CdSe}$  quantum dots for photovoltaic applications. *Nanoscale Res Lett* 2011, **6**:340.
12. Chen YX, Wei L, Zhang GH, Jiao J: Open structure  $\text{ZnO}/\text{CdSe}$  core/shell nanoneedle arrays for solar cells. *Nanoscale Res Lett* 2012, **7**:516.
13. Chen J, Lei W, Deng WQ: Reduced charge recombination in a co-sensitized quantum dot solar cell with two different sizes of  $\text{CdSe}$  quantum dot. *Nanoscale* 2011, **3**:674.
14. Chen C, Xie Y, Ali G, Yoo SH, Cho SO: Improved conversion efficiency of  $\text{Ag}_2\text{S}$  quantum dot-sensitized solar cells based on  $\text{TiO}_2$  nanotubes with a  $\text{ZnO}$  recombination barrier layer. *Nanoscale Res Lett* 2011, **6**:462.
15. Kieven D, Dittrich T, Belaidi A, Tornow J, Schwarzborg K, Allsop N, Lux-Steiner M: Effect of internal surface area on the performance of  $\text{ZnO}/\text{In}_2\text{S}_3/\text{CuSCN}$  solar cells with extremely thin absorber. *Appl Phys Lett* 2008, **92**:153107.
16. Wang LD, Zhao DX, Su ZS, Shen DZ: Hybrid polymer/ $\text{ZnO}$  solar cells sensitized by  $\text{PbS}$  quantum dots. *Nanoscale Res Lett* 2012, **7**:106.
17. Maiti N, Im SH, Lim CS, Seok SI: A chemical precursor for depositing  $\text{Sb}_2\text{S}_3$  onto mesoporous  $\text{TiO}_2$  layers in nonaqueous media and its application to solar cells. *Dalton Trans* 2012, **41**:11569.
18. Liu YB, Zhou HB, Li JH, Chen HC, Li D, Zhou BX, Cai WM: Enhanced photoelectrochemical properties of  $\text{Cu}_2\text{O}$ -loaded short  $\text{TiO}_2$  nanotube

array electrode prepared by sonoelectrochemical deposition. *Nano-Micro Lett* 2010, **2**:277.

19. Wu J, Wang ZM, Dorogan VG, Li SB, Zhou ZH, Li HD, Lee JH, Kim ES, Mazur YI, Salamo GJ: **Strain-free ring-shaped nanostructures by droplet epitaxy for photovoltaic application.** *Appl Phys Lett* 2012, **101**:043904.
20. Yafit I, Olivia N, Miles P, Gary H: **Sb<sub>2</sub>S<sub>3</sub>-sensitized nanoporous TiO<sub>2</sub> solar cells.** *J Phys Chem C* 2009, **113**:4254.
21. Moon SJ, Itzhaik Y, Yum JH, Zakeeruddin SM, Hodes G, Gratzel M: **Sb<sub>2</sub>S<sub>3</sub>-based mesoscopic solar cell using an organic hole conductor.** *J Phys Chem Lett* 2010, **1**:1524.
22. Im SH, Kim HJ, Rhee JH, Lim CS, Seok SI: **Performance improvement of Sb<sub>2</sub>S<sub>3</sub>-sensitized solar cell by introducing hole buffer layer in cobalt complex electrolyte.** *Energy Environ Sci* 2011, **4**:2799.
23. Han QF, Chen L, Zhu WC, Wang MJ, Wang X, Yang XJ, Lu LD: **Synthesis of Sb<sub>2</sub>S<sub>3</sub> peanut-shaped superstructures.** *Mater Lett* 2009, **63**:1030.
24. Lee YL, Chang CH: **Efficient polysulfide electrolyte for CdS quantum dot-sensitized solar cells.** *J Power Sources* 2008, **185**:584.
25. Seol M, Ramasamy E, Lee J, Yong K: **Highly efficient and durable quantum dot sensitized ZnO nanowire solar cell using noble-metal-free counter electrode.** *J Phys Chem C* 2011, **115**:22018.

doi:10.1186/1556-276X-8-89

**Cite this article as:** Li et al.: Annealing effect on Sb<sub>2</sub>S<sub>3</sub>-TiO<sub>2</sub> nanostructures for solar cell applications. *Nanoscale Research Letters* 2013 **8**:89.

**Submit your manuscript to a SpringerOpen<sup>®</sup> journal and benefit from:**

- ▶ Convenient online submission
- ▶ Rigorous peer review
- ▶ Immediate publication on acceptance
- ▶ Open access: articles freely available online
- ▶ High visibility within the field
- ▶ Retaining the copyright to your article

---

Submit your next manuscript at ▶ [springeropen.com](http://springeropen.com)

---